Out-of-plane stability of buckling-restrained braces including their connections

T. Takeuchi, R. Matsui & T. Tada
Tokyo Institute of Technology, Japan

K. Nishimoto
Nippon Steel Engineering Co., Ltd., Japan

SUMMARY:
Buckling-restrained braces (BRBs) are widely used in seismic countries as ductile seismic-resistant elements and energy dissipating elements. One of the key limits of BRBs is overall flexural buckling, and they are required to exhibit stable hysteresis under cyclic axial loading with out-of-plane drifts, their stability under such conditions being essential. However, many researches are indicating that there are risks of overall buckling including connections before the BRBs yield. In this paper, the stability conditions of BRBs including their connections are discussed based on cyclic loading tests with out-of-plane drifts, and a unified simple equation for evaluating their stability is proposed.

Keywords: Buckling-restrained brace, Connections, Cyclic loading, Buckling, Stability condition

1. INTRODUCTION

Buckling-restrained braces (BRBs) are expected to exhibit stable hysteresis under cyclic axial loading with out-of-plane drifts, and their stability under such conditions is essential. However, many researchers have indicated that there are risks of overall buckling including connections before the braces yields, when plastic hinges are introduced at the ends of the restrainers (Fig.1.1). In this paper, the stability conditions of BRBs including their connections are discussed and equations evaluating such conditions are proposed. Cyclic axial loading tests of BRBs with initial out-of-plane drift are carried out, and the validity of the proposed equation is confirmed.

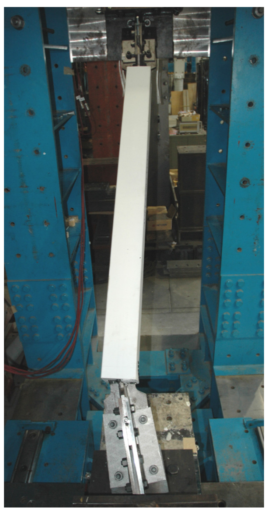

Figure 1.1. Overall Buckling of BRB including connections

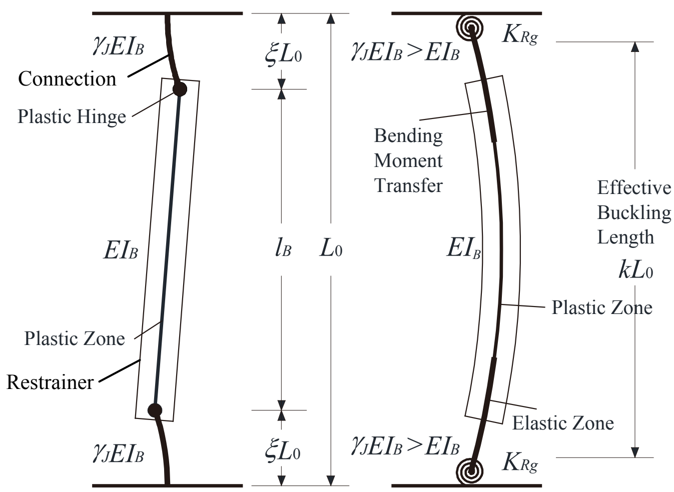

(a) Plastic Hinge Concept (b) Bending Moment Transfer

Figure 2.1. BRB Stability Condition

2. STABILITY CONDITION FOR BRBS INCLUDING CONNECTIONS

In AIJ Recommendation for Stability Design of Steel Structures (2009), following two concepts for BRB design to sustain stability including connections are indicated, as shown in Fig.2.1.

1) Plastic hinges are allowed at the restrainer-ends, and the stability conditions are given for the restrained part and connections individually [Fig.2.1(a)].
2) Bending moment transfer is expected at the restrainer-ends, and composite stability of the restrained part and connections is confirmed [Fig.2.1(b)]. Pin-ends types are included in this category.

For the concept 1), the following equations are proposed by Kinoshita et.al (2007).
The stability condition of the restrained part;

$$M_y^B \geq \frac{a_r N_{cu}}{1 - N_{cu}/N_{cr}^B} \tag{2.1}$$

The stability condition of connections;

$$N_{cr}^J = \frac{(1-2\xi)\pi^2 \gamma_J EI_B}{(2\xi L_0)^2} > N_{cu} \tag{2.2}$$

where, M_y^B: bending strength of the restrainer; a_r: expected imperfections; sum of a (restrainer imperfection), e (axial force eccentricity), and s_r (clearance between core and restrainer); N_{cu} : maximum axial force of core plates, normally estimated 1.2-1.5 times of yield force of the core plate including hardening; N^B_{cr} : Euler buckling strength of the restrainer; $\gamma_J EI_B$: Bending stiffness of the connections; and ξL_0 : connection length.
This concept is based on the condition that the ends of the connections are rigidly fixed against rotation; however, very stiff gusset plates are required to satisfy this condition. For example, a stiffened gusset plate as in Fig.2.2 (c) is essential. Moreover, preventing the rotation of the beam where BRBs are connected, large stiffening beam in out-of-plane directions are required as shown in Fig.2.3.
The other design concept of BRBs is the transfer of bending moment at the restrainer-ends as in the concept 2) in AIJ recommendation, which confirm the stability of the restrained part and the connections compositely as shown in Fig.2.1(b). Tekeuchi et.al (2009) indicated that the restrainer-ends can transfer the bending moment up to the bending strength of the restrainer or stiffened core section, if the stiffened ends of the core plates are inserted into the restrainer by more than two times the core plate width ($L_{in} > 2B_c$ in Fig.2.4(a)). Where, they produce an initial imperfection $a_r = a + e + s_r + (2s_r / L_{in})\xi L_0$ (Fig.2.4(b)) and the process of overall buckling can be described by a simple model as in Fig. 2.5.
As in the figures, the BRB are modelled as a bending element with rotational springs K_{Rg} (K_{Rg} = 0 for pin-ends) at both ends and initial imperfection a_r. When the bending moment reaches the bending strength of the restrainer-ends M_p^r, the brace collapses. Firstly, the ends of the connections are assumed to be rigid ($K_{Rg} = \infty$) and out-of-plane deformations of the connections in the mechanism phase are assumed to be cosine curves as in Fig.2.5(a);

$$y = \frac{a_r}{\xi L_0} + y_r \left[1 - \cos\left(\frac{\pi x}{2\xi L_0} \right) \right] \tag{2.3}$$

Then the strain energy stored in both connection is;

$$U_\varepsilon = 2\int_0^{\xi L_0} \frac{\gamma_J EI}{2} \left(\frac{d^2 y}{dx^2} \right)^2 dx = \frac{\pi^4 \gamma_J EI y_r^2}{32(\xi L_0)^3} \tag{2.4}$$

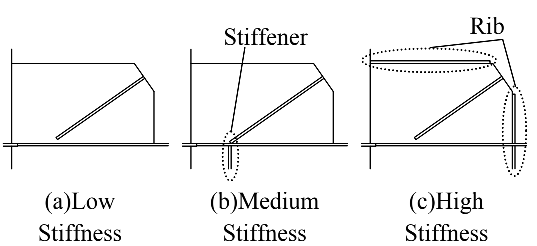

Figure 2.2. Connection with various stiffness

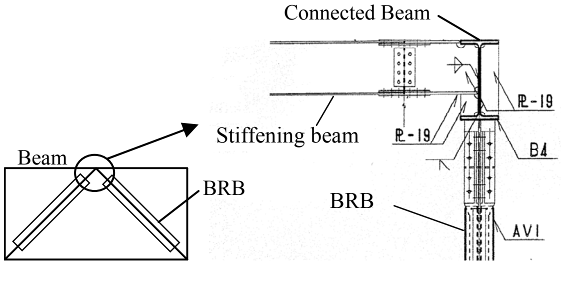

Figure 2.3. Rotational stiffener at BRB connections

The rotation angle of the plastic hinges is;

$$\Delta\theta_r = \left.\frac{dy}{dx}\right|_{x=\xi L_0} - \frac{a_r}{\xi L_0} = \frac{\pi}{2\xi L_0} y_r \tag{2.5}$$

Then the plastic strain energy stored in the hinges are;

$$U_p = 2M_p^r \Delta\theta_r = \frac{\pi y_r}{\xi L_0} M_p^r \tag{2.6}$$

The axial deflection is;

$$\Delta u_g = 2 \cdot \frac{1}{2} \int_0^{\xi L_0} \left[\left(\frac{dy}{dx} \right)^2 - \left(\frac{a_r}{\xi L_0} \right)^2 \right] dx = \frac{\pi^2 y_r^{\,2}}{8\xi L_0} + \frac{2a_r y_r}{\xi L_0} \tag{2.7}$$

The work done is;

$$T = N\Delta u_g = \frac{\pi^2 (y_r^2 + 16a_r y_r / \pi^2)}{8\xi L_0} N \tag{2.8}$$

with the principle of stationary total potential energy;

$$\frac{\partial (U_\varepsilon + U_p - T)}{\partial y_r} = \frac{\pi^4 \gamma_J EI y_r}{16(\xi L_0)^3} + \frac{\pi y_r}{\xi L_0} M_p^r - \frac{\pi^2 (y_r^2 + 16a_r y_r / \pi^2)}{8\xi L_0} N_{cr} = 0 \tag{2.9}$$

$$N_{cr} = \frac{\pi^2 \gamma_J EI y_r}{(2\xi L_0)^2} \frac{y_r}{y_r + 8a_r / \pi^2} + \frac{4M_p^r}{\pi(y_r + 8a_r / \pi^2)} \tag{2.10}$$

Approximating $8/\pi^2$ as 1, we obtain the following.

$$N_{cr} \approx \frac{\pi^2 \gamma_J EI}{(2\xi L_0)^2} + \frac{4}{\pi} \frac{M_p^r}{y_r + a_r} \tag{2.11}$$

Similar calculation can be carried out in an asymmetrical mode as shown in Fig.2.5(b), as follows.

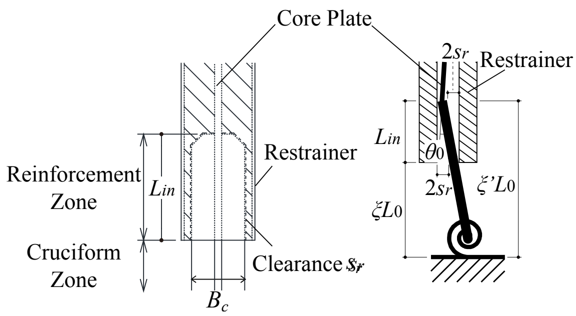

(a) Detail (b) Model

Figure 2.4. Bending Moment Transfer at Restrainer End

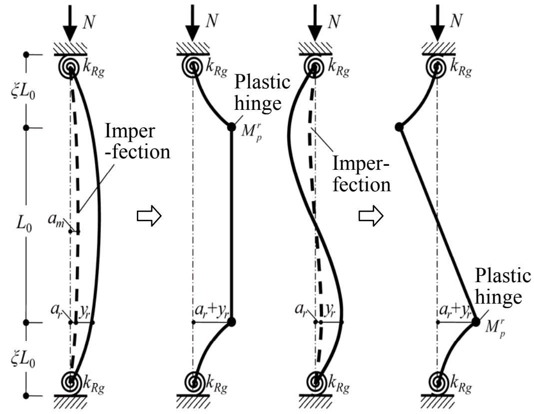

(a) Symmetric mode (b) Asymmetric mode

Figure 2.6. Assumed Process of Overall Buckling

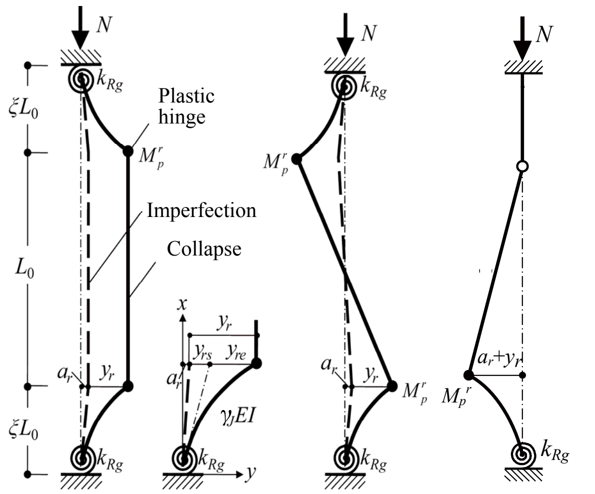

(a) Symmetrical (b) Asymmetrical (c) One-side

Figure 2,5. Overall Buckling with Rotational Springs

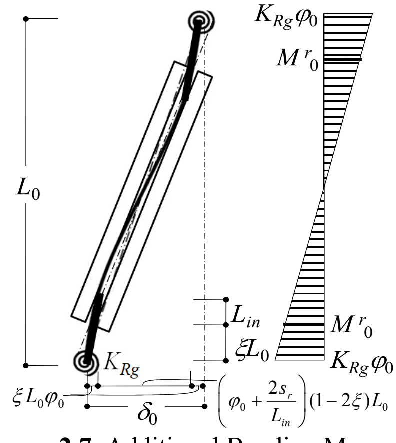

Figure 2.7. Additional Bending Moment by Out-of-plane Drift

$$U_p = \frac{\pi y_r}{\xi L_0}\frac{\pi - 2\pi\xi + 4\xi}{1-2\xi}M_p^r \tag{2.12}$$

$$T \approx \frac{\pi^2 N}{8\xi(1-2\xi)L_0}(y_r^2 + 16\xi a_r y_r / \pi^2) \tag{2.13}$$

$$N_{cr} = \frac{\pi^2(1-2\xi)\gamma_J EIy_r}{(2\xi L_0)^2}\frac{y_r}{y_r + 8a_r/\pi^2} + \frac{4(1-2\xi+4\xi/\pi)}{\pi(y_r + 8a_r/\pi^2)}M_p^r \tag{2.14}$$

When $\xi = 0.25$, it can be approximated as follows:

$$N_{cr} \approx \frac{\pi^2(1-\xi 2)\gamma_J EI}{(2\xi L_0)^2}\frac{y_r}{y_r + a_r} + \frac{M_p^r}{y_r + a_r} \tag{2.15}$$

When $M_p^r = 0$ and $a_r \ll y_r$, Eq.(2.15) approaches Eq.(2.2). As indicated by Eqs.(2.11) and (2.15), the overall buckling strength is determined by the asymmetrical mode when the ends of the connections are rigidly fixed.

Next, consider rotational stiffness K_{Rg}. Define normalized rotational stiffness κ_{Rg} as follows:

$$\kappa_{Rg} = \frac{K_{Rg}\xi L_0}{\gamma_J EI} \tag{2.16}$$

As in Fig.2.5(a), additional deformation by the rotation of the end spring is defined as y_{rs}. As deformation by connection bending y_{re} become equivalent to y_{rs} when $\kappa_{Rg} = 3$, the strain energy stored in the springs is estimated as;

$$U_\varepsilon = \frac{\pi^4 \gamma_J EI y_r^{\,2}}{32(\xi L_0)^3}\left(\frac{\kappa_{Rg}}{\kappa_{Rg}+3}\right)^2 \tag{2.17}$$

The spring rotation $\Delta\theta_s$, plastic hinge rotation $\Delta\theta_r$, and axial deformation can be expressed as follows:

$$\Delta\theta_s = \frac{y_r}{\xi L_0}\frac{3}{\kappa_{Rg}+3} \tag{2.18}$$

$$\Delta\theta_r = \frac{\pi y_r}{2\xi L_0}\frac{\kappa_{Rg}}{\kappa_{Rg}+3} + \frac{y_r}{\xi L_0}\frac{3}{\kappa_{Rg}+3} = \frac{y_r}{2\xi L_0}\frac{\pi\kappa_{Rg}+6}{\kappa_{Rg}+3} \tag{2.19}$$

$$\Delta u_g = \frac{y_r^2 + 2a_r y_r}{\xi L_0}\left(\frac{1}{2}\frac{3}{\kappa_{Rg}+3} + \frac{\pi^2}{16}\frac{\kappa_{Rg}}{\kappa_{Rg}+3}\right) = \frac{y_r^2 + 2a_r y_r}{\xi L_0}\frac{\pi^2}{8}\frac{\kappa_{Rg}+24/\pi^2}{\kappa_{Rg}+3} \tag{2.20}$$

Then the energy stored in the springs and hinges and the works done can be evaluated, respectively;

$$U_s = \frac{\gamma_J EI y_r \kappa_{Rg}}{(\xi L_0)^3}\left(\frac{3}{\kappa_{Rg}+3}\right)^2 \tag{2.21}$$

$$U_p = \frac{y_r}{\xi L_0}\frac{\pi\kappa_{Rg}+6}{\kappa_{Rg}+3}M_p^r \tag{2.22}$$

$$T = \frac{\pi^2(y_r^2 + 2a_r y_r)}{8\xi L_0}\frac{\kappa_{Rg}+24/\pi^2}{\kappa_{Rg}+3}N \tag{2.23}$$

From the condition $\partial(U_\varepsilon + U_p - T)/\partial y_r = 0$,

$$N_{cr} \approx \frac{\pi^2 \gamma_J EI y_r}{(2\xi L_0)^2}\cdot\frac{\kappa_{Rg}}{\kappa_{Rg}+24/\pi^2}\cdot\frac{y_r}{y_r + a_r} + \frac{4}{\pi}\cdot\frac{M_p^r}{y_r + a_r}\cdot\frac{\kappa_{Rg}+6/\pi}{\kappa_{Rg}+24/\pi^2} \tag{2.24}$$

In the above equation (2.24) become Eq.(2.25) when the connection ends are pinned ($\kappa_{Rg} = 0$).

$$N_{cr} = \frac{M_p^r}{y_r + a_r} \tag{2.25}$$

On contrary, Eq.(2.11) can be restored when $\kappa_{Rg} = \infty$. Hence Eq.(2.24) covers symmetrical buckling strength for various rotational stiffness from pin-ends to rigid-ends.

Asymmetrical strength can be derived by similar process as;

$$N_{cr} \approx \frac{\pi^2(1-2\xi)\gamma_J EI y_r}{(2\xi L_0)^2}\cdot\frac{\kappa_{Rg}}{\kappa_{Rg}+24/\pi^2}\cdot\frac{y_r}{y_r + a_r} + \frac{M_p^r}{y_r + a_r} \tag{2.26}$$

Similarly, strength for one-side buckling mode as shown in Fig.2.5(c) can be derived as follows.

$$N_{cr} \approx \frac{\pi^2(1-2\xi)\gamma_J EI}{(2\xi L_0)^2} \frac{{}_\xi\kappa_{Rg}}{(1-\xi)({}_\xi\kappa_{Rg}+24/\pi^2)} \frac{y_r}{y_r+a_r} + \frac{M_p}{y_r+a_r} \tag{2.27}$$

Eqs.(2.26), (2.27) approaches Eq.(2.25) when κ_{Rg} = 0 and Eq.(2.15) when κ_{Rg} = ∞, also covering asymmetrical buckling strength for various rotational stiffness. Eq.(2.26) gives slightly lower values than Eq.(2.27). Eqs.(2.24), (2.26) and (2.27) all indicate that the axial force decreases as the out-of-plane displacement y_r increases. When the elastic axial force and out-of-plane displacement relationship expressed by Eq. (2.28) reaches this condition, the brace is considered to be collapsed [Fig.2.6(a)].

$$N = \frac{y_m}{a_m+y_m} N_{cr}^B = \frac{y_r}{a_r+y_r} N_{cr}^B \tag{2.28}$$

where, $N_{cr}{}^B$ is overall elastic buckling strength which can be derived as follows.

$$\begin{cases} N_{cr}^B = \dfrac{4\pi^2 EI}{L_0{}^2} \cdot \dfrac{{}_L\kappa_{Rg}^2 + 10\,{}_L\kappa_{Rg} + 16}{{}_L\kappa_{Rg}^2 + 14\,{}_L\kappa_{Rg} + 64} \\ {}_L\kappa_{Rg} = K_{Rg} \dfrac{L_0}{EI} \end{cases} \tag{2.29}$$

Substituting $y_r = a_r N/(N_{cr}^B - N)$ into Eq. (2.26), the required bending strength $M_p{}^r$ can be derived as follows:

$$M_p^r = \frac{a_r}{1-N/N_{cr}^B}\left[N - \frac{\pi^2(1-2\xi)\gamma_J EIy_r}{(2\xi L_0)^2} \cdot \frac{{}_\xi\kappa_{Rg}}{{}_\xi\kappa_{Rg}+24/\pi^2} \cdot \frac{y_r}{y_r+a_r}\right] = \frac{a_r}{1-N/N_{cr}^B}\left[N - N_{cr}^r\right] \tag{2.30}$$

When the structure deforms out-of-direction not only axial deformation, additional bending moment is distributed as in Fig.2.7. The initial bending moment at the restrainer-end $M_0{}^r$ can be estimated as;

$$M_0^r = (1-2\xi)K_{Rg}\left[\frac{\delta_0}{L_0} - \frac{2s_r(1-2\xi)}{L_{in}}\right] \geq 0 \tag{2.31}$$

where, δ_0 is expected story drift in an out-of-plane direction.
Bending moment strength at restrainer-ends are considered to be reduced by this initial moment.
Consequently, the stability condition can be expressed as follows, with the condition that the cross point of Eqs.(2.28) and (2.30) (see Fig.2.8) exceeds the expected maximum axial force N_{cu}.

$$M_p^r - M_0^r \geq \frac{a_r}{1-N_{cu}/N_{cr}^B}\left(N_{cu} - N_{cr}^r\right) \quad \text{where,} \quad M_p^r - M_0^r \geq 0 \tag{2.32}$$

where, $M_p{}^r$:Ultimate bending strength of restrainer-ends, $M_0{}^r$: Initial bending moment at restrainer- ends [Eq.(2.31)], a_r: Initial imperfections $= a + e + s_r + (2s_r / L_{in})\xi L_0$, N_{cu}: Expected maximum axial force of BRB = Yield force multiplied by hardening factor, $N^B{}_{cr}$: Elastic overall buckling strength [Eq.(2.29)], $N^r{}_{cr}$: Elasto-plastic buckling strength caused by connections using the following equivalent slenderness ratio by Eq.(2.33). In this equation (2.33), ξ' in Fig.2.4(b) instead of ξ should be used estimating plastic hinges can be produced at the neck of the reinforced zone of the core plate.

$$\lambda_r = \frac{2\xi' L_0}{i} \cdot \sqrt{\frac{{}_\xi\kappa_{Rg} + 24/\pi^2}{(1-2\xi')\,{}_\xi\kappa_{Rg}}} \tag{2.33}$$

where $N^r{}_{cr}$ must satisfy the following limit to preventing the yield at outer ends of the gusset plates:

$$N_{cr}^r \leq N_p^g = \frac{1}{a_r}\left[M_{pc}^g - \frac{M_0^r}{(1-2\xi')}\right] \tag{2.34}$$

where, $M_{pc}{}^g$: Bending strength of the outer ends of the gusset plates including the effect of axial force.
To satisfy Eq.(2.32), two approaches can be used for BRB design.

1)Decrease $M_0{}^r$ and $N^r{}_{cr}$, by decreasing κ_{Rg}, and provide enough bending strength $M_p{}^r$ at the restrainer-end. This concept corresponds to transferring bending moment at the restrainer-ends. [Fig.2.1(b)].

2)When κ_{Rg} is large, the left part of Eq.(2.32) becomes small or zero, so satisfy Eq.(2.32) by designing $N^r{}_{cr}$ larger than N_{cu}. This concept corresponds to Eq.2 which allows hinges at the restrainer-ends. [Fig.2.1(a)].

As above, Eq.(2.32) covers both design concepts discussed in Fig.2.1.

3. CYCLIC LOADING TEST OF BRB WITH OUT-OF-PLANE DISPLACEMENT

To confirm the stability including the connections, cyclic loading tests of the BRB with out-of-plane displacement are carried out. The test configuration with specimens is shown in Figs.3.1 and 3.2, the loading program are shown in Fig.3.3, and the test matrix is shown in Table 3.1. The core plates are JIS-SN400B (average yield strength: 270MPa) 12mm thick and 90mm wide, the restrainers are mortar in-filled box section of 125mm square and 2.3mm thick or circular tube of 139.8 dia. and 3.2mm thick. The insert length of the stiffened part of the core plates into the restrainers L_{in} can be 180mm, 90mm, 45mm, which is 2.0 times, 1.0 times and 0.5 times of the core width, respectively. In addition, the clearance between the core plate and the restrainers are varied from 1.0mm to 2.0mm, and 6 different specimens are tested. The specimens are labelled as M-(R:Requtangular, C:Circular)-L(Insert length ratio) -S-(Clearance). The same gusset plates are used in all specimen which have a small rotational stiffness (κ_{Rg}≈0.04). Initial imperfection angles in each specimen are summarized in Table 3.2.

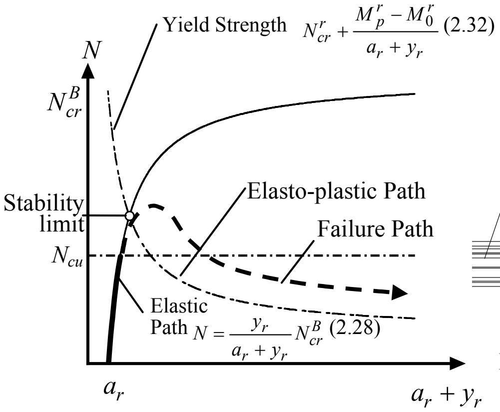

Figure 2.8. Load-Deflection Relationship

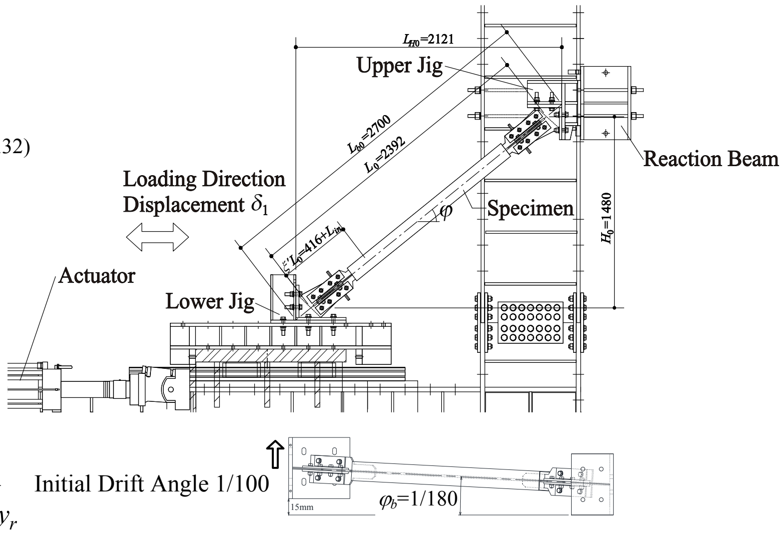

Figure 3.1. Cyclic Loading Test Setup

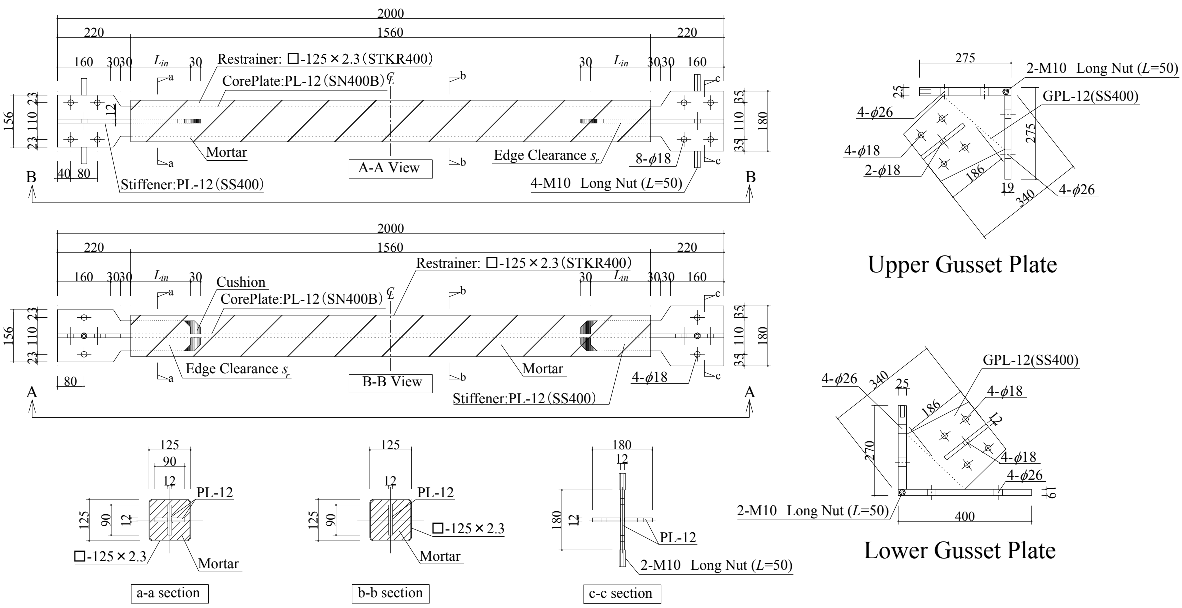

Figure 3.2. Test Specimen

Table 3.1. Test Matrix

Specimen	A_c (mm^2)	σ_{cy} (N/mm^2)	EI (Nmm)	σ_{ry} (N/mm^2)	K_{Rg} (Nmm)	$\gamma_J EI$ (Nmm)	L_0 (mm)	ξL_0 (mm)	ξ	$\xi' L_0$ (mm)	ξ'
MRL2.0S1	1080	266.8	5.81×10^{11}	385.8	9.73×10^{7}	1.20×10^{12}	2392	416	0.17	596	0.25
MRL2.0S2				391.5							
MCL2.0S2		269.7	7.14×10^{11}	365.7							
MRL1.0S1		266.8	5.81×10^{11}	391.5						506	0.21
MRL1.0S2											
MCL1.0S2		269.7	7.14×10^{11}	365.7							

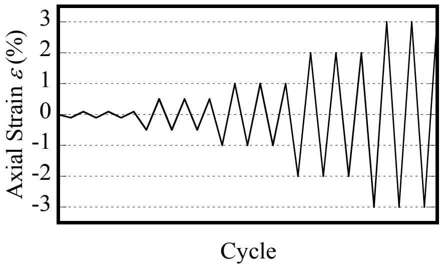

Figure 3.3. Loading Protocol

Table 3.2. Initial Imperfection Angle

Specimen	L_{in} (mm)	s_r (mm)	$\theta_0 = L_{in} / s_r$ (rad)
MRL2.0S1	180	1	0.01
MRL2.0S2		2	0.02
MCL2.0S2			
MRL1.0S1	90	1	0.02
MRL1.0S2		2	0.04
MCL1.0S2		2	

Before the test, out-of-plane deformation equivalent to the story drift of 1% radian is applied to each specimen, and then axial cyclic deformation equivalent up to 1-3% of the plastic length of the core plate is applied. This normalized axial strain is roughly equivalent to in-plane story drift angle. The hysteresis loops obtained for each specimen are shown in Fig.3.4 to Fig.3.10.

MRL2.0S1 (Fig.3.4) showed stable hysteresis up to 12 cycles of 3% normalized strain, until out-of-plane instability appeared. This performance is considered to be satisfactory for energy-dissipation braces. MRL2.0S2 (Fig.3.5) which has slightly larger initial imperfection than previous one, showed stable hysteresis until 3 cycles up to 3% normalized strain, then out-of-plane instability appeared. MCL2.0S2 (Fig.3.6) is constituted by a circular mortar in-filled steel tube, showed stable hysteresis until 2 cycle up to 2% normalized strain, until appearance of out-of-plane instability. MRL1.0S1 (Fig.3.7) reached the yield strength of the core plate and showed stable hysteresis up to the 2nd cycle of 1.0% normalized strain, then experienced overall buckling hinged at the restrainer-ends. MRL1.0S2 (Fig.3.8 and Fig.3.10) showed a hysteresis loop for only one cycle of 0.5% normalized strain, then experienced overall buckling hinged at the restrainer-ends. MCL1.0S2 (Fig.3.9) exhibited a hysteresis loop for only one cycle of 0.5 normalized strain, then undergoes overall buckling hinged at the restrainer-ends.

4. COMPARISON WITH THE PROPOSED EQUATION

These test results indicate that the stabilities of BRBs are strongly affected by the insert length ratio and clearance, which is expected from the proposed Eq.(2.32). In the following, each specimen is evaluated using Eq.(2.32). For the evaluation, bending strength of each specimen at the restrainer-ends M_p^r needs to be estimated. Takeuchi et.al (2009) proposed the following equations for the tested types of BRB:

$$M_p^r = \min\left\{M_p^{core}, M_p^{rest}\right\} \tag{4.1}$$

M_p^{rest} represents the bending strength of the restrainer end as follows:

$$M_p^{rest} = \begin{cases} \min\left\{Z_{rp}\sigma_{ry}, K_{Rr1}\theta_{y1}' + K_{R2}\left(\theta_{y2} - \theta_{y1}'\right)\right\} & (\text{Rectangular Tube}) \\ \min\left\{Z_{rp}\sigma_{ry}, K_{Rr1}\theta_{y}\right\} & (\text{Circular Tube}) \end{cases} \tag{4.2}$$

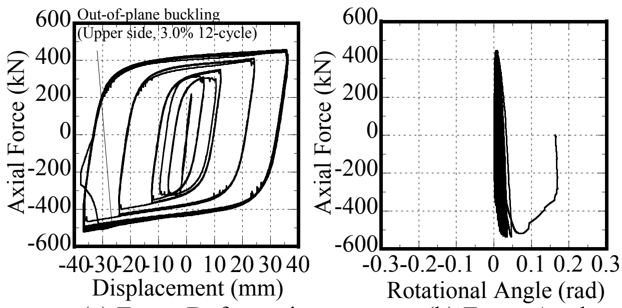

(a) Force-Deformation (b) Force-Angle

Figure 3.4. MRL2.0S1

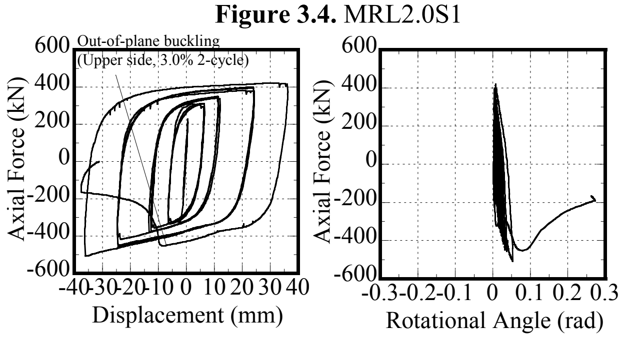

(a) Force-Deformation (b) Force-Angle

Figure 3.5. MRL2.0S2

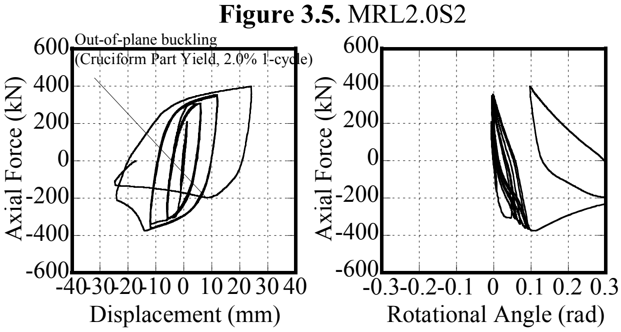

(a) Force-Deformation (b) Force-Angle

Figure 3.6. MCL2.0S2

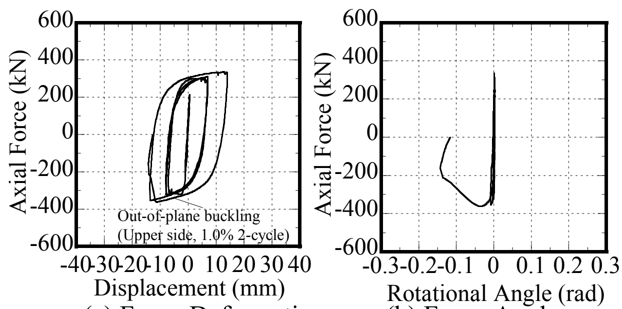

(a) Force-Deformation (b) Force-Angle

Figure 3.7. MRL1.0S1

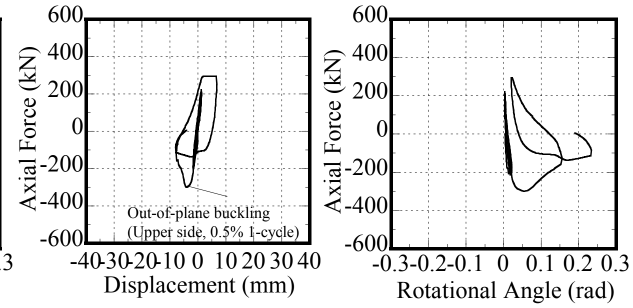

(a) Force-Deformation (b) Force-Angle

Figure 3.8. MRL1.0S2

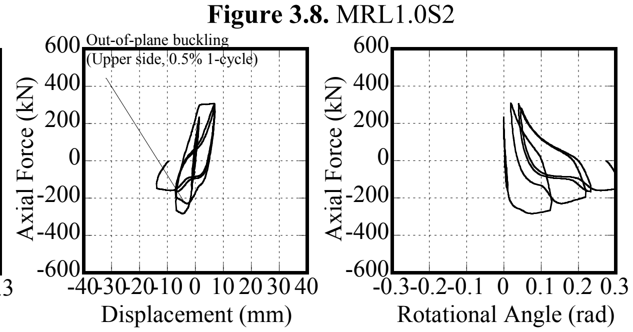

(a) Force-Deformation (b) Force-Angle

Figure 3.9. MCL1.0S2

Table 4.1. Bending Capacities at the Restrainer Ends

Specimen	Yield Strength of Cruciform Zone (Nmm)	Yield Strength of Restrainer (Nmm)	$M_p{}^r$ (Nmm)
MRL2.0S1	4.33×10^6	1.26×10^7	4.31×10^6
MRL2.0S2		5.71×10^6	
MCL2.0S2	4.38×10^6	2.38×10^7	4.38×10^6
MRL1.0S1	4.33×10^6	1.43×10^6	1.43×10^6
MRL1.0S2			
MCL1.0S2	4.38×10^6	6.51×10^6	4.38×10^6

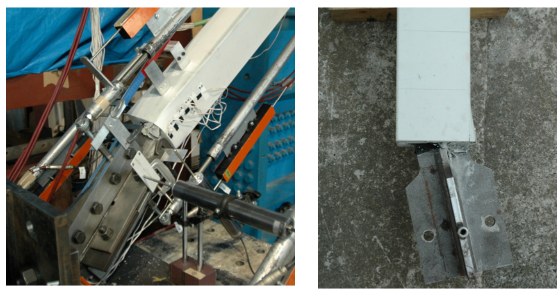

(a) Buckling (b) Buckling Zone

Figure 3.10. MRL1.0S2 Collapse Mode

where, Z_{rp} is the plastic section modulus of the restrainer, σ_{ry} is the yield stress of the restrainer, K_{Rr1} is the elastic rotational stiffness at the restrainer-ends, θ_{y1}' is the pseudo initial yield angle for the rectangular restraint tube, K_{Rr2} is the rotational stiffness at the restrainer-ends after yielding, θ_{y2} is the angle that plastic hinge occurs, and θ_y is the yield angle for the circular restraint tube.

$M_p{}^{core}$ represents the bending strength of the cruciform core plate as follows:

$$M_p^{core} = \left\{1-\left(\frac{N_{cu}-N_{wy}^c}{N_u^c-N_{wy}^c}\right)^2\right\}Z_{cp}\sigma_{cy} \tag{4.3}$$

where, N_{cu} is the maximum axial force of the core plate, N_{wy}^c is the yield axial force of the cruciform core plate at the web zone, N_{cu} is the ultimate strength of the core plate, Z_{cp} is the plastic section modulus of the core plate, and σ_{cy} is the yield stress of the core plate. The study indicates that M_p^r is decided the cruciform section whose strength given by Eq.(4.3) when the insert length ratio exceeds around 2.0. The obtained values of M_p^r in each specimen are summarized in Table 4.1. The conditions for each specimen are evaluated using the safety Index of Eq.(4.4), and the results are summarized in Table 4.2. Out of six specimens, only MRL2.0S1 satisfies the condition, for which safety indices given by;

$$(M_p^r - M_0^r)\Big/\left[\frac{a_r}{1-N_{cu}/N_{cr}^B}\left(N_{cu}-N_{cr}^r\right)\right] \tag{4.4}$$

is 1.11. The safety index of MRL2.0S2 and MCL2.0S2 is 0.62 and 0.68 respectively, which is slightly

Table 4.2. Stability Evaluations using the Proposed Equation

Specimen	N_{cr}^B (kN)	a_r (mm)	N_{cu} (kN)	N_{cr}^r (kN)	M_0^r (kNm)	Safety Index	Experimantal Result
MRL2.0S1	1158	6.8	432	82	0.09	1.11	3.0%-12cycle
MRL2.0S2		12.4			0.00	0.62	3.0%-2cycle
MCL2.0S2	1389		437			0.68	1.0%-2cycle
MRL1.0S1	1158	11.4	432	111		0.24	0.5%-1cycle
MRL1.0S2		21.7				0.13	0.5%-1cycle
MCL1.0S2	1389		437			0.43	0.5%-1cycle

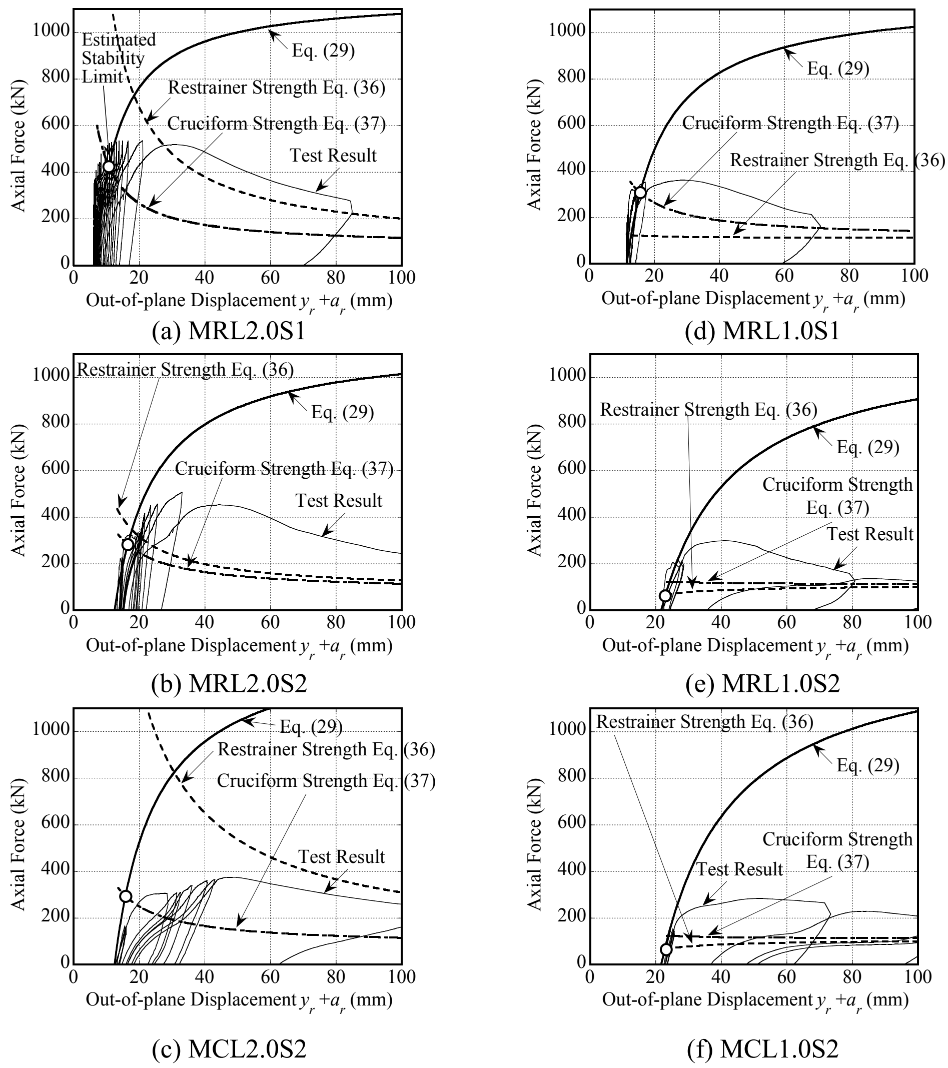

(a) MRL2.0S1 (d) MRL1.0S1

(b) MRL2.0S2 (e) MRL1.0S2

(c) MCL2.0S2 (f) MCL1.0S2

Figure 4.1. Axial Force vs. Out-of-plane Displacement

unsatisfactory from Eq.(2.32). All other specimens have much lower values, which indicate that their overall stabilities are not guaranteed. In total, the given safety values satisfactory estimate the performance of each specimen obtained in the cyclic loading tests and therefore are considered to be valid. Fig.4.1 shows the measured axial force-displacement relationships compared with the equations discussed in Sec.2. The test results are well estimated by the proposed equations so the proposed equations are considered to be valid.

5. CONCLUSIONS

The overall stabilities of BRBs are discussed and confirmed by cyclic loading test with out-of-plane displacement. The conclusions reached are summarized as follows.

1) The stability conditions for BRBs can be expressed by a single equation using a simple hinge model with end springs. This equation covers both design concepts of BRBs discussed in AIJ recommendation 2009.
2) In the cyclic loading tests, specimens with lesser insert length at the restrainer-ends experience overall buckling before achieving stable hysteresis, which is not satisfactory as the standard performance of a BRB. In contrast, specimens with larger insert length showed stable hysteresis up to 3%
3) The proposed equation explains well the performance of each specimen in the test, and is considered to be valid.

AKCNOWLEDGEMENT

The authors would like to acknowledge that the research is supported by Nippon Steel Engineering Co. Ltd., and JFE Engineering Co. Ltd.

REFERENCES

Architectural Institute of Japan (2009) **Recommendation for Stability Design of Steel Structures**, **Sec.3.5** Buckling Restrained Braces.

Takeuchi, T., Yamada, S., Kitagawa, M., Suzuki, K., and Wada, A. (2004) Stability of Buckling Restrained Braces Affected by the Out-of-plane Stiffness of the Joint Element, **Journal of Structure and Constructional Engineering**, **575**, 121-128 (in Japanese)

Kinoshita, T., Koetaka, Y., Inoue, K. (2007): Criteria of Buckling Restrained Braces to Prevent Out-of-plane Buckling, **Journal of Structure and Constructional Engineering**, **21**, 141-148 (in Japanese)

Chou, C. C., Chen, P. J. (2009) Compressive behavior of central gusset plate connections for a buckling-restrained braced frame, **Journal of Constructional Steel Research**, **65**, 1138-1148

Matsui, R., Takeuchi, T., Nishimoto, K., Takahashi, S., and Ohyama, T. (2010) Effective Buckling Length of Buckling Restrained Braces Considering Rotational Stiffness at Restrainer Ends, **7th International Conference on Urban Earthquake Engineering & 5th International Conference on Earthquake Engineering** Proceedings, 1049-1058

Hikino, T., Okazaki, T., Kajiwara, K., Nakashima, M. (2011) Out-of-Plane stability of buckling-restrained braces, **Proceeding of Structural Congress, ASCE, 2011**